



Performance optimization of a double-effect desalination unit integrated in a steam power plant of a chemical factory

Fathia Hafdhi^{a,*}, Tahar Khir^b, Ali Ben Yahya^c, Ammar Ben Brahim^a

^aApplied Thermodynamic Research Laboratory LR18ES33, University of Gabes, National Engineering School of Gabes, Omar Ibn Khattab Street, 6029 Gabes, Tunisia, Tel. +216 29 277 683; email: hafdhi.fathia@gmail.com (F. Hafdhi), Tel. +216 23 025 464; email: ammar.benbrahim@enig.rnu.tn (A.B. Brahim)

^bModelisation, Mechanic, Energy and Material Research Unit UR17ES48, National Engineering School of Gabes, Omar Ibn Khattab Street, 6029 Gabes, Tunisia, Tel. +216 93 222 458; email: taherkhir@yahoo.fr

^cTunisian Chemical Group (TCG), B.P. 72 – Gabes 6000, Tunisia, Tel. +216 98 444 935; email: benyahia.ali@gct.com.tn

Received 29 August 2017; Accepted 14 January 2019

ABSTRACT

An energetic and exergetic optimization of a double-effect thermal vapor compression desalination system is performed. This unit is integrated in the thermal power plant of phosphoric acid factory owned by The Tunisian Chemical Group. The daily production of this unit is about 528 m³ of fresh water. A mathematical model based on energy and exergy balances is established using EES software. The effects of the main operating parameters on the desalination unit performances are analyzed. Obtained results show that the maximum exergy efficiency is obtained for the evaporator 2 followed by the distillate and brine pumps. The condenser has the lowest exergy efficiency. The thermocompressor is the major contributor in exergy destruction. The mass flow rate and the pressure of the motive steam affect positively the gain output ratio, while the last one decreases slightly with the motive steam temperature. In order to preserve suitable overall exergy efficiency, the motive steam temperature should be taken between 152°C and 154°C, which corresponds to motive steam pressure between 4.4 and 4.7 bar. These ranges constitute optimum operating conditions.

Keywords: Energy; Exergy; Optimization; Double-effect desalination; Power plant

1. Introduction

The Tunisian Chemical Group (TCG) constitutes the most industrial pole in the country. The main activities of this group are to produce the phosphoric acid and fertilizers from crude phosphate. For this reason, several chemical industrial factories are built in different regions. This represents an important factor for the Tunisian economic balance. Although the economic importance of the phosphate industry, the investment and operating costs of the different plants remain very substantial. To overcome this problem, the TCG conducts programs in the purpose to optimize the production cost and to reduce the energy consumption.

In the frame of this program, a thermodynamic analysis of a steam turbine power plant operating in a phosphoric acid factory owned by TCG is performed. This paper is focused on an energy and exergy optimization of a double-effect (DE) desalination unit constituting one of the important parts of the indicated power plant. The main object of this study is to define the optimum operating conditions leading to the maximum exergy efficiency of the DE thermal vapor compression (DE-TVC).

The multi-effect TVC (ME-TVC) is considered as one of the best technologies of desalination systems. Several works have been carried out on the ME-TVC optimization; among them, we found the following:

* Corresponding author.

Sadri et al. [1] performed a mathematical model of multi effect desalination with thermal vapor compression (MED-TVC) reverse osmosis (RO) hybrid desalination plant installed in Iran. The material, energy, and exergy equations governing the behavior of fluid flow in the different compound systems are developed. Moreover, the thermodynamic properties of each stream are determined taking into account the boiling point elevation (BPE), which permits to determine the performances of the desalination unit. A multi-objective optimization for different configurations of hybrid systems are established in the aim to select the best one leading to a higher permeate production and exergy efficiency as well as a suitable gain output ratio (GOR). Obtained results show that the multi effect desalination (MED) part engenders the maximum of exergy destruction rate, especially in the TVC followed by the first effect. On the other hand, the permeate flow production is increased by 34% in the hybrid system compared with the MED unit. Furthermore, the RO unit and MED system exergy efficiencies are increased to reach 8.63% and 12.84%, respectively, in the hybrid configuration.

Al-Mutaz et al. [2] performed an optimization of the thermocompressor suction location in MED-TVC desalination systems. The study is focused on the effect of the thermocompressor suction position on the desalination plant performances. A mathematical model is established in the purpose to determine the optimum location leading to suitable values of entrainment ratio (ER), GOR, specific heat transfer area, and energy consumption.

Almutairi et al. [3] conducted an energetic and exergetic optimization of a cogeneration combined power plant and an ME-TVC-MED desalination unit under several operating conditions. The developed model of the plant is performed using IPSEpro software. The obtained results showed that the higher exergy destruction rate of the considered plant occurs in the combustor. In order to improve the plant performances, authors suggest to operate in full load and with a lower ambient temperature. Moreover, an increase of pressure ratio is recommended. In the desalination side, the obtained results showed that the main sources of irreversibility are located in the effects and the thermocompressor of about 78.7%. The increase of the effect numbers leads to an enhancement of the exergetic efficiency by about 0.7%, while the raise of the feed water temperature allows slight increase in the exergetic efficiency. On other hand, an ER close to unit is recommended in the aim to obtain a higher performance and capacity of the cogeneration plant.

Bataineh [4] investigates the overall performance of an MED-TVC plant motivated by a solar steam generation located in Aqaba, Jordan, with a daily production of about 50,000 m³. The mathematical model established by EES software allows determining the influence of operational and conceptual parameters on the plant performances. The results demonstrate that the system efficiency increases with augmentation of the first effect temperature. Furthermore, a collector orientation along a north-south axis with an area around 1,080,000 m² and a storage size of about 75 L/m² leads to an optimum plant performance.

B. Ortega-Delgado et al. [5] performed a parametric study of an MED-TVC plant coupled with a Rankine cycle power unit installed in Trapani, Italy. A mathematical model was developed and validated for the plant using EES software.

The effect of operating parameters on the plant performances was established. The main results drawn from this study reveal that a higher GOR was reached for a higher motive steam pressure and for a steam ejector location close to the last effect. The produced distillate decreases by reducing the pressure of motive steam and increasing the suction pressure.

Azimibavil et al. [6] performed a dynamic simulation of a MED system by solving partial differential equations governing the fluid behavior outside tube bundle. The appropriate equation of heat transfer process was established taking into account the correlations related to the evaporation on outside tube area as well as the condensation inside them. Authors found that the condensation of feeding steam inside tubes occurs linearly. Moreover, for a steady-state behavior, an unexpected interruption in steam feed for 200 s, the process requires approximately 550 s to return to normal situations. Furthermore, a reduction of feed water until the half of nominal values leads to an increase of brine concentration that accentuates the threat of tube fouling.

An exergetic analysis of multi stage flash (MSF) distillation plant is established by Al Ghamdi et al. [7]. This plant is installed at Yanbu Saudi Arabia. A mathematical model based on mass, energy, and exergy balances is developed and simulated using MATLAB code. This study investigates the plant performance at normal and peak loads. The exergy destruction rate of different system compound is determined, and the heat recovery section is the major resource of irreversibility rate. The obtained exergy efficiency of the plant is quite and around 3%. Authors confirm that the increase of the effect number leads to a decrease in the exergy destruction rate. Furthermore, authors compare between once through and brine mixing (MSF-M) design. Obtained results confirm that the (MSF-M) is the best choice.

Experimental study was carried out by Ghalavand et al. [8] on a humidification-dehumidification desalination system based on specific design. The gas humidification occurred by direct contact with hot water. Then the obtained air is compressed and cooled in order to recuperate the humidity as desalinated water. The effects of the operating parameters such as inlet temperatures, pressure, water fraction, and condenser temperature on the plant performances are analyzed. Authors found that higher values of the two stream inlet temperatures lead to maximum fresh water production and GOR of the desalination unit. The optimum value of water to air ratio giving the best performances is equal to 2.

Mazini [9] developed a dynamic mathematical model for an MED-TVC system. Mass and energy balances are established. The dynamic and static behaviors in the different compounds of the plant are modeled and simulated by MATLAB/SIMULINK software. The suggested model is validated using real operating data of Kish Island plant installed in Iran. Furthermore, this model is investigated with modifying operating conditions and applying disruption in the system behavior. The obtained results show a good performance of the proposed model.

A comparative performance study between three desalination system configurations was carried out by Al-Mutaz et al. [10]. A mathematical model based on material and energy balances was conducted for each configuration systems. This work aims to investigate, for each configuration, the influence of design and operating parameters on

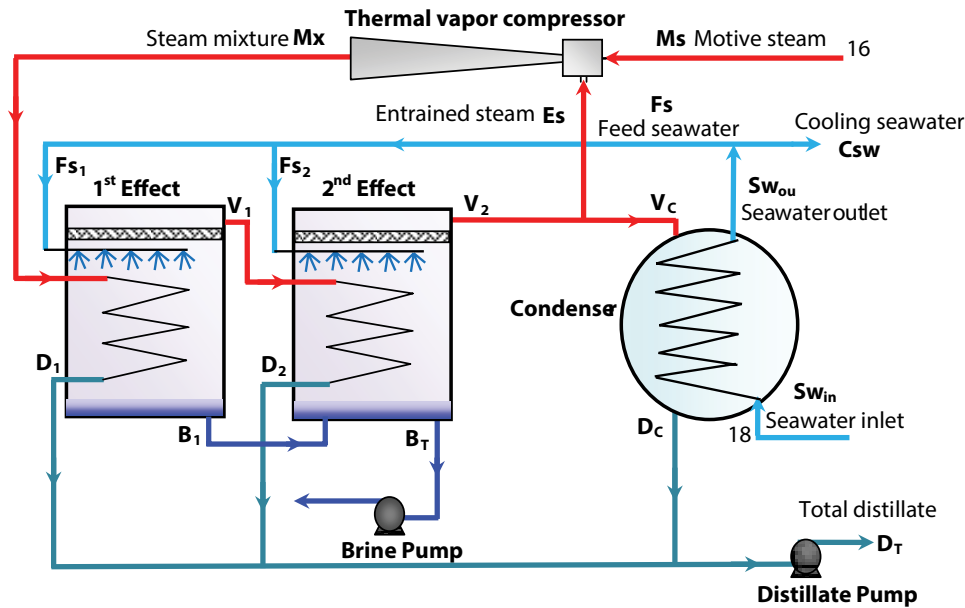


Fig. 2. Double effect with thermal vapor compressor desalination unit.

528 m³. The main components of studied system are TVC, two effects, and a shell and tube seawater cooled condenser. The motive steam (Ms) passes through the ejector entraining the flux (Es) to reach the operating conditions of the first evaporator. The steam mixture (Mx) follows through the tube bundle to be condensed under the effect of seawater stream (Fs₁). The condensation latent heat is used to evaporate part of Fs₁. The produced vapor (V₁), constituting the thermal source of the second evaporator, is condensed and then shifted by the distillate pump. The first evaporator brine (B₁) is introduced to the next effect at lower pressure and temperature. A flash evaporating process is then produced in the second effect. This small quantity of vapor is added to the produced steam (V₂) due to seawater evaporation (Fs₂).

The obtained vapor (V₂) is divided into two main fluxes: the first one (Es) is entrained by the TVC while the second (V_c) is transferred to the condenser. Therefore, seawater is preheated through the condenser before feeding the evaporators. The total fresh water is transferred by distillate pump to the storage tank, and the total brine is rejected to sewers. The operating parameters of DE-TVC are given in Table 1.

3. Energetic and exergetic analysis

3.1. Mathematical model

A steady-state mathematical model of the DE desalination unit with TVC was established based on the mass, energy, heat transfer equations, and exergy balances applied to each component of the unit considering the following assumptions [1,7]:

- All processes are assumed operating at a steady state.
- The kinetic and potential exergies are neglected.
- The dead state was considered as $P_0 = 1.013$ bar and $T_0 = 293.15$ K.
- No chemical reaction occurred in the different processes.

Table 1
Specifications of the DE-TVC unit

Parameters	Values
Effects number	2
Motive steam (t/h)	5.4
Intake seawater (t/h)	109
Feed seawater (t/h)	102
Cooling seawater (t/h)	7
Total brine output (t/h)	88
Capacity of DE-TVC (t/d)	22
Temperature of the vapor in the first effect (°C)	56
Pressure of the vapor in the first effect (bar)	0.15
Temperature of the vapor in the second effect (°C)	51
Pressure of the vapor in the second effect (bar)	0.12
Temperature of condensation (°C)	48
Pressure of condensation (bar)	0.11
Gain output ratio	3.9

- Thermodynamic losses are neglected.
- The distillate is salt free.

As known, exergy is the maximum useful work which can be extracted from a system as it reversibly comes into equilibrium with its environment. The total exergy is expressed as follows [16]:

$$\dot{E}_x = \dot{E}_{ph} + \dot{E}_{ch} + \dot{E}_{ke} + \dot{E}_p \quad (1)$$

Taking into account the assumptions, the total exergy is equal to

$$\dot{E}_x = \dot{E}_{ph} + \dot{E}_{ch} \quad (2)$$

Physical exergy is given by [17]

$$\dot{E}_{ph} = \dot{m}_i \left[(h_i - h_0) - T_0 (s_i - s_0) \right] \quad (3)$$

Chemical exergy is expressed as follows [17]:

$$E\dot{x}_{ch} = \dot{m} \left[\sum_{i=1}^n X_i \text{ex}_{ch,i} + RT_0 \sum_{i=1}^n X_i \ln(X_i) \right] \quad (4)$$

The temperature difference between two effects DT is calculated by [1]

$$\Delta T = T_1 - T_2 \quad (5)$$

The brine temperature (T_i) in each effect is equal to the vapor saturation temperature plus the BPE due to the dissolved salts in the water, given by [1,5]:

$$T_i = T_{vi} + \text{BPE} \quad (6)$$

The BPE is calculated according to the following equation [18]:

$$\text{BPE} = X(A + BX + CX^2) \quad (7)$$

with $A = (8.325 \times 10^{-2} + 1.883 \times 10^{-4}T + 4.02 \times 10^{-6}T^2)$,

$B = (-7.625 \times 10^{-4} + 9.02 \times 10^{-5}T - 5.2 \times 10^{-7}T^2)$, and

$C = (1.522 \times 10^{-4} - 3 \times 10^{-6}T - 3 \times 10^{-8}T^2)$,

where T is the temperature ($^{\circ}\text{C}$) and X is the salt weight percentage. The above equation is valid over the following ranges: $1 \leq X \leq 16\%$; $10 \leq T \leq 180^{\circ}\text{C}$.

The condensation of the vapor generated in the first evaporator i occurs in the second one $i + 1$ at temperature T_{ci} which is lower than the boiling temperature in the first evaporator due to the thermodynamic losses. The condensation temperature is expressed by [5]

$$T_{ci} = T_i - \text{BPE} - \Delta T_{ti} \quad (8)$$

The saturation temperature of the generated vapor in the first effect decreases by a total amount defined as [5,16]

$$\Delta T_{ti} = \Delta T_{mi} + \Delta T_{pipe i} + \Delta T_{cond i} \quad (9)$$

The different terms of Eq. (9) represent [5,18]:

Temperature drop in the demister:

$$\Delta T_{mi} = T_{vsat,i} - T'_{vsat,i} \quad (10)$$

Temperature drop in the connecting pipes:

$$\Delta T_{pipe i} = T'_{vsat,i} - T_{ci} \quad (11)$$

Temperature drop in the evaporator:

$$\Delta T_{cond i} = T'_{ci} - T_{ci} \quad (12)$$

where $T_{vsat,i}$ and $T'_{vsat,i}$ are the saturation temperatures before and after the demister, T_{ci} is the saturation temperature inside the tube bundle in the heat transfer process, and T'_{ci} is the saturation inlet vapor temperature of the second evaporator.

Mass, energy, and exergy balances of the different components are established in the following paragraphs.

3.1.1. Evaporator 1

The first effect flow diagram is illustrated in Fig. 3.

Mass balance:

Seawater side

$$\dot{m}_{Fs_1} = \dot{m}_{V_1} + \dot{m}_{B_1} \quad (13)$$

$$x_{Fs_1} \dot{m}_{Fs_1} = x_{B_1} \dot{m}_{B_1} \quad (14)$$

Energy balance:

$$\dot{m}_{Mx} (h_{Mx} - h_{D_1}) = \dot{m}_{Fs_1} Cp_{Fs_1} (T_{B_1} - T_{Fs_1}) + \dot{m}_{V_1} L_{V_1} \quad (15)$$

The heat flux through the first effect can be determined as follows:

$$Q_{ev1} = U_{ev1} A_{ev1} (T_{Mx} - T_{ev1}) \quad (16)$$

Therefore, the heat transfer area A_{ev1} is obtained by

$$A_{ev1} = \frac{\dot{m}_{Mx} (h_{Mx} - h_{D_1})}{U_{ev1} (T_{Mx} - T_{ev1})} \quad (17)$$

The overall heat transfer coefficient U_{ev1} can be calculated as [18]

$$U_{ev1} = \frac{(1939.4 + 1.40562 \times T_{ev1} - 0.0207525 \times T_{ev1}^2 + 0.0023186 \times T_{ev1}^3)}{1000} \quad (18)$$

Exergy balance:

$$\dot{E}_{D,Evap1} = \dot{m}_{Mx} \left[(h_{Mx} - h_{D_1}) - T_0 (s_{Mx} - s_{D_1}) \right] - \dot{m}_{Fs_1} Cp_{Fs_1} \left[(T_{B_1} - T_{Fs_1}) - T_0 \ln \frac{T_{B_1}}{T_{Fs_1}} \right] - \dot{m}_{V_1} L_{V_1} \left(1 - \frac{T_0}{T_{V_1}} \right) \quad (19)$$

The amount of steam produced in the first effect is calculated according to the energy balance, given:

$$\dot{m}_{V_1} = \frac{\dot{m}_{Mx} (h_{Mx} - h_{D_1}) - \dot{m}_{Fs_1} Cp_{Fs_1} (T_{B_1} - T_{Fs_1})}{L_{V_1}} \quad (20)$$

3.1.2. Evaporator 2

The evaporator 2 flow diagram is presented in Fig. 4.

Mass balance:

Seawater side

$$\dot{m}_{Fs_2} + \dot{m}_{B_1} = \dot{m}_{V_2} + \dot{m}_{B_2} \quad (21)$$

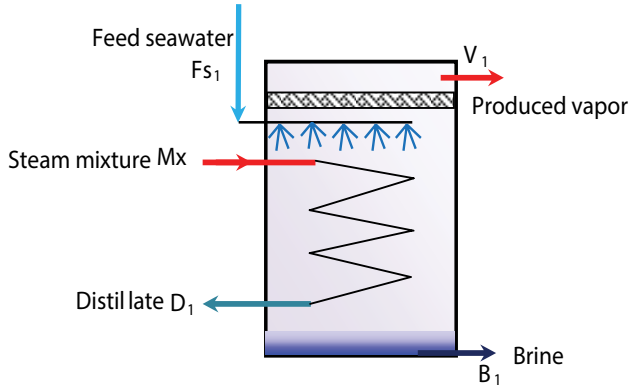


Fig. 3. First effect flow diagram.

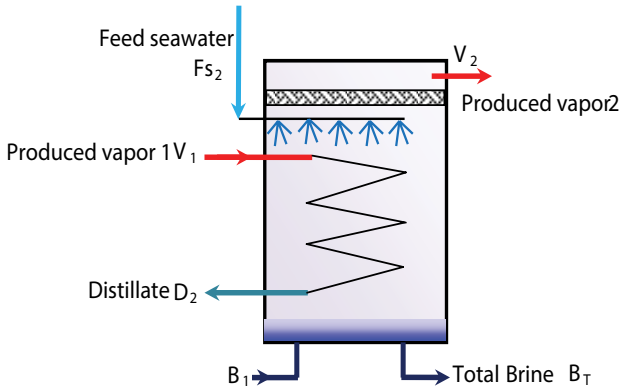


Fig. 4. Second effect flow diagram.

$$x_{F_{s2}} \dot{m}_{F_{s2}} + x_{B_1} \dot{m}_{B_1} = x_{B_T} \dot{m}_{B_T} \quad (22)$$

Energy balance:

$$\dot{m}_{V_1} (h_{V_1} - h_{D_2}) + \dot{m}_{B_1} Cp_{B_1} (T_{B_T} - T_{B_1}) = \dot{m}_{F_{s2}} Cp_{F_{s2}} (T_{B_T} - T_{F_{s2}}) + \dot{m}_{V_2} L_{V_2} \quad (23)$$

The heat flux through the second effect can be determined as follows:

$$Q_{ev2} = U_{ev2} A_{ev2} (T_{V_1} - T_{ev2}) \quad (24)$$

Therefore, the heat transfer area A_{ev2} is calculated by

$$A_{ev2} = \frac{\dot{m}_{V_1} (h_{V_1} - h_{D_2})}{U_{ev2} (T_{V_1} - T_{ev2})} \quad (25)$$

The Eq. (26) is used to determine the heat transfer coefficient U_{ev2} considering the temperature T_{ev2} :

$$U_{ev2} = \frac{(1939.4 + 1.40562 \times T_{ev2} - 0.0207525 \times T_{ev2}^2 + 0.0023186 \times T_{ev2}^3)}{1000} \quad (26)$$

Exergy balance:

$$\begin{aligned} \dot{E}_{D,EvapII} = & \dot{m}_{V_1} L_{V_1} \left(1 - \frac{T_0}{T_{V_1}} \right) + \dot{m}_{B_1} Cp_{B_1} \left[(T_{ev1} - T_{ev2}) - T_0 \ln \frac{T_{B_1}}{T_{B_T}} \right] - \\ & \dot{m}_{F_{s2}} Cp_{F_{s2}} \left[(T_{ev2} - T_{F_{s2}}) - T_0 \ln \frac{T_{ev2}}{T_{F_{s2}}} \right] - \dot{m}_{V_2} L_{V_2} \left(1 - \frac{T_0}{T_{V_2}} \right) \end{aligned} \quad (27)$$

The amount of steam produced in the second effect is calculated as follows:

$$\dot{m}_{V_2} = \frac{\dot{m}_{V_1} (h_{V_1} - h_{D_2}) - \dot{m}_{F_{s2}} Cp_{F_{s2}} (T_{B_T} - T_{F_{s2}}) + \dot{m}_{B_1} Cp_{B_1} (T_{B_T} - T_{B_1})}{L_{V_2}} \quad (28)$$

3.1.3. Thermocompressor

The TVC is a steam ejector used to create vacuum by the expansion of motive steam at high pressure through a divergent. This permits to entrain another stream of vapor at low pressure. This technology is widely used in water desalination plants due to its reliability and simplicity in operating and maintenance. The ER is the main parameter characterizing the thermocompressor performance, and it is defined as the ratio of motive steam mass flow rate to the entrained vapor (Ms/Es). Several methods are available to determine this parameter. In the actual study, the semi-empirical model developed by El-Desouky [16,19] is considered for which the ER is expressed as follows:

$$ER = 0.296 \times \left(\frac{P_{Mx}}{P_{Es}} \right)^{1.19} \times \left(\frac{P_{Ms}}{P_{Es}} \right)^{0.015} \times \left(\frac{PCF}{TCF} \right) \quad (29)$$

where P_{Mx} and P_{Es} are the pressures of compressed steam and entrained vapor, respectively, and calculated as

$$P_{Mx} = 1000 \times \exp \left(\frac{-3892.7}{T_{Mx} + 273.15 - 42.6776} + 9.5 \right) \quad (30)$$

$$P_{Es} = 1000 \times \exp \left(\frac{-3892.7}{T_{Es} + 273.15 - 42.6776} + 9.5 \right) \quad (31)$$

Furthermore, correction factors are defined for the motive steam pressure and entrained vapor temperature as follows [18]:

$$PCF = 3 \times 10^{-7} (P_{Ms})^2 - 0.0009 (P_{Ms}) + 1.6101 \quad (32)$$

$$TCF = 2 \times 10^{-8} (T_{Es})^2 - 0.0006 (T_{Es}) + 1.0047 \quad (33)$$

These equations are valid for the following ranges: $ER \leq 4$; $10^\circ\text{C} < T_{Es} \leq 500^\circ\text{C}$; $100 \leq P_{Ms} \leq 3,500 \text{ kPa}$ and $6 \leq \frac{P_{Mx}}{P_{Es}} \leq 1.81$.

The thermocompressor flow diagram is illustrated in Fig. 5.

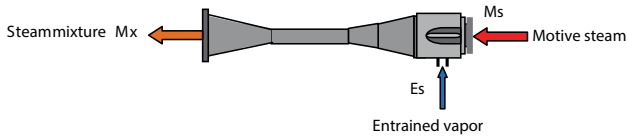


Fig. 5. Thermocompressor flow diagram.

Mass balance:

$$\dot{m}_{Mx} = \dot{m}_{Ms} + \dot{m}_{Es} \quad (34)$$

Energy balance:

$$\dot{m}_{Mx} h_{Mx} = \dot{m}_{Ms} h_{Ms} + \dot{m}_{Es} h_{Es} \quad (35)$$

Exergy balance:

$$\dot{E}_{D,thc} = \dot{m}_{Ms} [(h_{Ms} - h_{Mx}) - T_0 (S_{Ms} - S_{Mx})] - \dot{m}_{Es} [(h_{Mx} - h_{Es}) - T_0 (S_{Mx} - S_{Es})] \quad (36)$$

3.1.4. Condenser

The condenser flow diagram is shown in Fig. 6.

Mass balance:

Shell side

$$\dot{m}_{Vc} = \dot{m}_{Dc} \quad (37)$$

Tube side

$$\dot{m}_{Sw_{in}} = \dot{m}_{Sw_{out}} \quad (38)$$

Energy balance:

$$\dot{m}_{Vc} L_{V2} = \dot{m}_{Sw_{in}} Cp_{Sw} (T_{Sw_{out}} - T_{Sw_{in}}) \quad (39)$$

The condensation latent heat of the steam V_c inside the condenser is calculated as follows:

$$\dot{m}_{Vc} L_{V2} = U_{cd} A_{cd} (LMTD)_{cd} \quad (40)$$

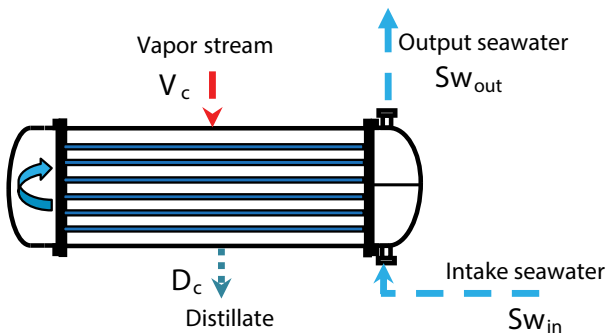


Fig. 6. Condenser flow diagram.

The heat transfer area of the condenser A_{cd} is determined by:

$$A_{cd} = \frac{\dot{m}_{Vc} L_{V2}}{U_{cd} (LMTD)_{cd}} \quad (41)$$

The overall heat transfer coefficient U_{cd} can be calculated as follows [18]:

$$U_{cd} = 1.7194 + (3.2063 \times 10^{-2} \times T_{V2}) - (1.5971 \times 10^{-5} \times T_{V2}^2) + (1.9918 \times 10^{-7} \times T_{V2}^3) \quad (42)$$

The logarithmic mean temperature difference (LMTD) is calculated as [20]

$$LMTD_{cd} = \frac{(T_{V2} - T_{Sw_{out}}) - (T_{Dc} - T_{Sw_{in}})}{\ln \left(\frac{T_{V2} - T_{Sw_{out}}}{T_{Dc} - T_{Sw_{in}}} \right)} \quad (43)$$

Exergy balance:

$$\dot{E}_{D,cd} = \dot{m}_{Vc} L_{V2} \left(1 - \frac{T_0}{T_{V2}} \right) - \dot{m}_{Sw_{in}} Cp_{Sw} \left((T_{Sw_{out}} - T_{Sw_{in}}) - T_0 \ln \frac{T_{Sw_{out}}}{T_{Sw_{in}}} \right) \quad (44)$$

The system performance of the DE-TVC has been evaluated by the following parameters:

Gain output ratio:

$$GOR = \frac{\dot{m}_{D_r}}{\dot{m}_{Ms}} \quad (45)$$

Specific heat transfer area:

$$sA = \frac{\sum_{i=1}^2 A_{evi} + A_{cd}}{\dot{m}_{D_r}} \quad (46)$$

Specific heat consumption:

$$sQ = \frac{\dot{m}_{Ms} L_{Ms}}{\dot{m}_{D_r}} \quad (47)$$

4. Results and discussion

The selected objective function for our investigation is to maximize the overall exergy efficiency of the whole system and to minimize the production cost of distilled water. A code is established using EES software permitting to perform all the required calculations.

As a first step and in the aim to validate the established model, a comparison between the calculated and the actual conceptual parameters of the DE-TVC system is carried out. Obtained results are arranged in Table 2. One can see that a good agreement is obtained between the calculated design

Table 2
Comparison between the conceptual and the calculated parameters

Component	Conceptual parameters [21]	Calculated parameters
Evaporator 1	Heat exchange area = 732 m ² Tubes number: 1,940	Heat exchange area = 731.8 m ² Tubes number: 1,925
Evaporator 2	Heat exchange area = 732 m ² Tubes number: 1,940	Heat exchange area 731.8 m ² Tubes number: 1,925
Condenser	Heat exchange area = 150 m ² Tubes number: 488	Heat exchange area = 149.9 m ² Tubes number: 481
sA (m ² s/kg)	281	279.9
GOR	3.9	3.84

parameters and the actual ones. This confirms the good accuracy of the established model.

Fig. 7 depicts the exergy efficiency of the different components of the DE-TVC unit. The maximum exergy efficiency is obtained for the EvapII followed by the distillate and brine pumps. Among the main components of the desalination system, the thermocompressor TVC presents exergy efficiency of about 56%. However, the condenser has the lowest exergy efficiency of 31.66%; this is due to the temperature gradient between the two streams.

The exergy destruction rates are represented in Fig. 8. The overall exergy input is about 1,121 kW. The total exergy destruction rate constitutes 73.3% of the provided exergy rate. Otherwise, the thermocompressor engenders the maximum irreversibility rate of about 533.5 kW. This represents about 65% of the total exergy destruction rate. This can be explained by the fact that major exergy input flux is used to feed this component (1,103 kW). This constitutes 98.4% of the overall exergy input. As expected, the minimum exergy destruction rates are created through the pumps.

In the following part, the effects of the main operating parameters on the whole desalination system and its components are presented.

The influences of the motive steam temperature T_s and pressure P_s on the thermocompressor exergy performances

are not widely analyzed in the previous works. In this study, the effects of these operating parameters are carried out.

The variations of exergy efficiency of thermocompressor according to motive steam temperature T_s are presented in Fig. 9. For T_s variation range, the exergy efficiency decreases by about 3.93%, while the irreversibility rate increases by about 10%. These results prove the importance of the motive steam temperature considered as key operating parameter.

The influences of the motive steam pressure P_s on the exergy performances of the same element are illustrated in Fig. 10. The increase of P_s from 3.4 to 6.2 bar leads to an enhancement of the exergy efficiency of about 3%.

The variation of exergy efficiency of the condenser according to seawater temperature is presented in Fig. 11. For a variation range of seawater temperature of 9°C, the exergy efficiency increases by about 53%. This must be taken into consideration during the different seasons.

Although there are positive effects of the seawater temperature on the condenser exergetic efficiency, the required heat transfer area is increased, as illustrated in Fig. 12. This causes the rising of the investment costs constituting a constraint that must be taken into consideration in the economic optimization.

Moreover, the increase of seawater temperature provokes a rise of the intake seawater mass flow rate as shown

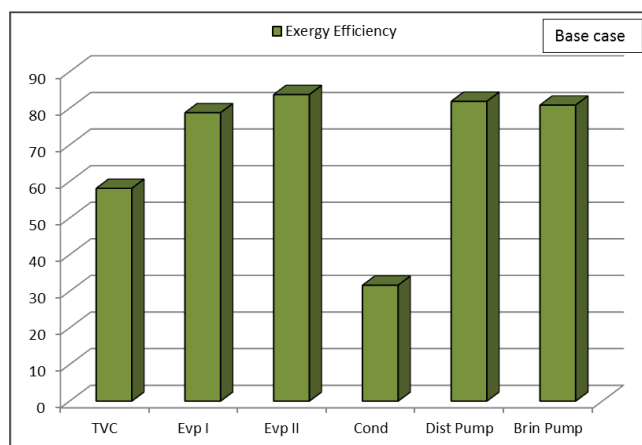


Fig. 7. Exergy efficiency of MED-TVC components.

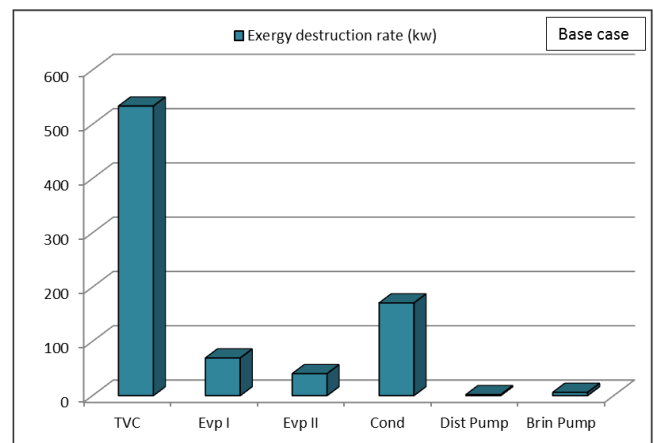


Fig. 8. Exergy destruction rate of MED-TVC components.

in Fig. 13. This can be explained by the decrease of the temperature difference between the two streams (steam and seawater). Indeed, for higher values of seawater temperature, an important cooling water mass flow rate is required.

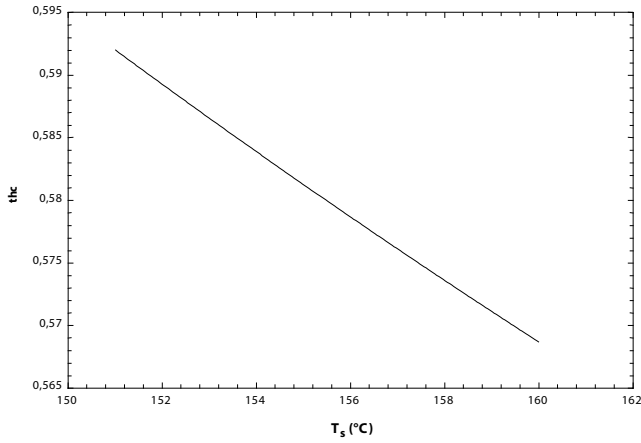


Fig. 9. Variation of thermocompressor exergy efficiency according to motive steam temperature.

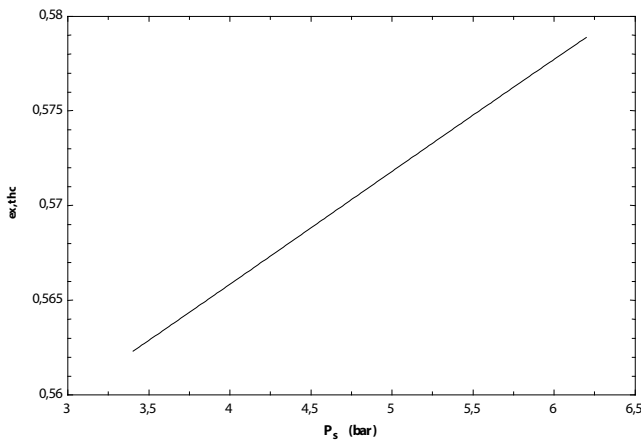


Fig. 10. Variation of thermocompressor exergy efficiency according to motive steam pressure.

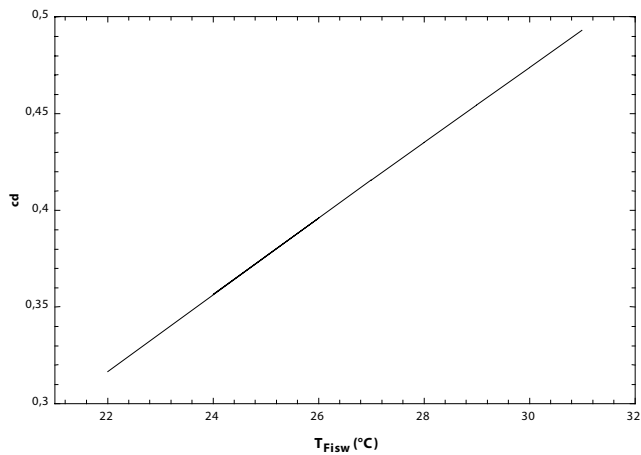


Fig. 11. Variation of condenser exergy efficiency according to intake seawater temperature.

The influence of the motive steam pressure on the distillate water production is illustrated in Fig. 14. The motive steam pressure affects slightly the fresh water production. Indeed, for P_s variation from 4.2 to 6 bar, the distillate increases by about 2.5%.

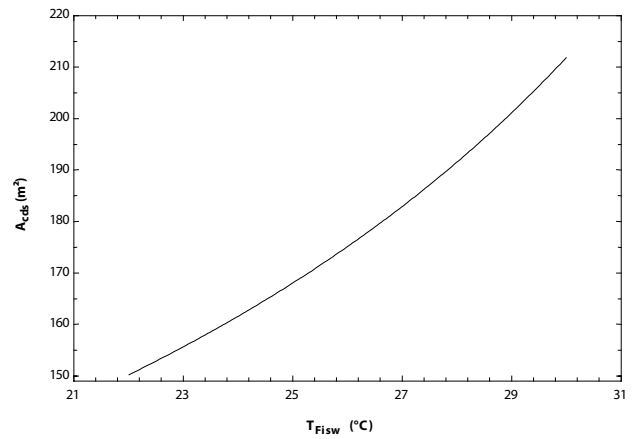


Fig. 12. Variation of condenser surface heat exchange according to intake seawater temperature.

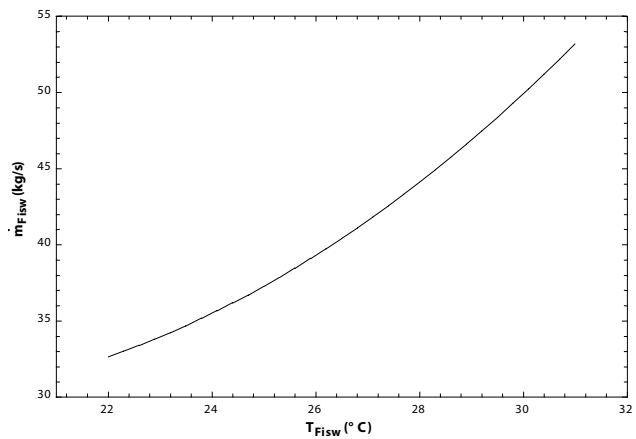


Fig. 13. Variation of seawater mass flow rate according to intake seawater temperature.

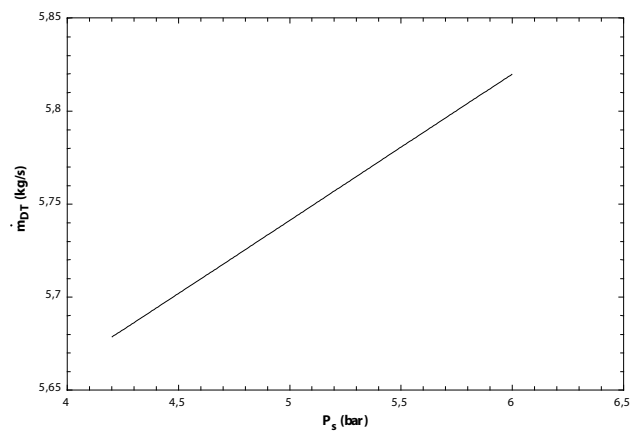


Fig. 14. Variation of distillate water according to motive steam pressure.

As defined by Eq. (45), a higher value of the GOR is desired for the desalination unit in order to obtain the maximum distillate mass flow rate. The variation of GOR according to the motive steam mass flow rate \dot{m}_s is presented in Fig. 15. For a variation range of \dot{m}_s from 0.972 to 1.694 kg/s, the GOR increases by about 7.54% to reach 3.891.

The variations of GOR according to the motive steam temperature for different values of \dot{m}_s are presented in Fig. 16. As indicated in Fig. 15, the GOR increases with \dot{m}_s , while it decreases slightly with the motive steam temperature. This can be explained by the fact that a part of input heat flux is used for sensible seawater heating. In addition, the latent heat is reduced at higher temperatures.

These results agree with the investigations of Al-Mutaz and Irfan [7]. Their obtained results show that for a variation range of the motive steam mass flow rate from 8 to 20 kg/s, the total distillate increases three times. Furthermore, Alasfour et al. [22] found that the GOR increases by about 11.23% according to the increase of the motive steam pressure from 5 to 28 bar for ME-TVC system. Besides, Ehsan et al. [19] show

that the GOR decreases by increasing the motive steam temperature for a MED unit coupled to a gas turbine plant.

The specific heat transfer area sA is one of the performance parameter of the MED unit. The variation of sA according to the motive steam mass flow rate is presented in Fig. 17.

The specific heat transfer area decreases sensibly with \dot{m}_s . Since the sA is defined as the ratio of the total heat transfer area to the distillate production and seeing that the distillate production increases with the enhancement of \dot{m}_s , the specific heat transfer area is consequently reduced.

Fig. 18 depicts the variation of the specific heat consumption \dot{Q}_s according to motive steam pressure. For the considered variation range of P_s (from 4.2 to 6 bar), \dot{Q}_s is reduced by about 2.44%. Alasfour et al. [22] have obtained a \dot{Q}_s reduction of 9.67% for a motive steam pressure varying from 5 to 28 bar.

The overall exergetic efficiency of the MED-TVC system is presented in Fig. 19 according to motive steam pressure. This efficiency is around 2.2% and slightly affected by P_s .

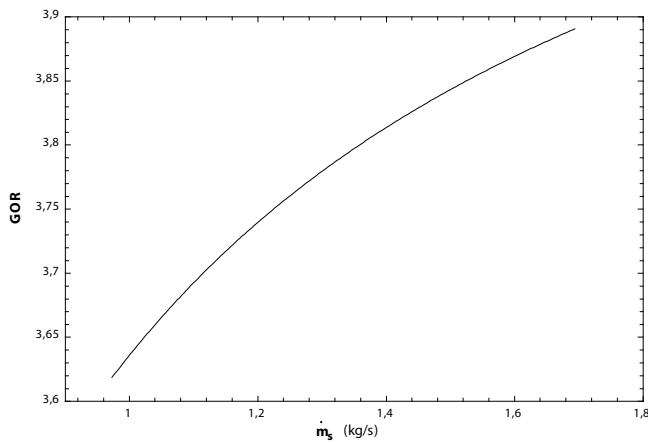


Fig. 15. Variation of GOR according to motive steam mass flow rate.

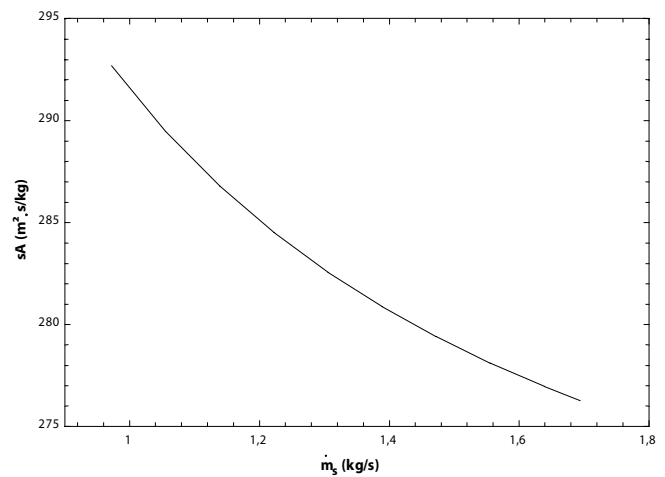


Fig. 17. Variation of specific heat transfer area according to motive steam mass flow rate.

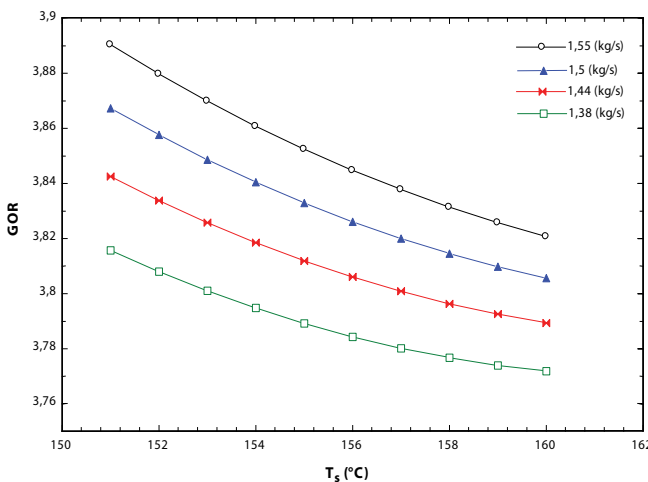


Fig. 16. GOR according to motive steam temperature for different \dot{m}_s .

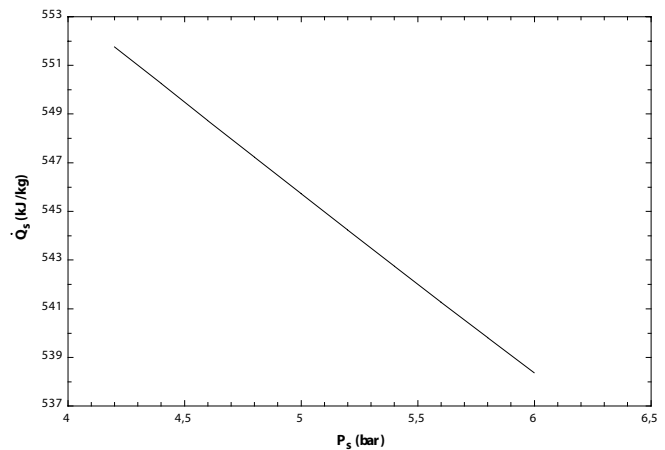


Fig. 18. Variation of specific heat consumption according to motive steam pressure.

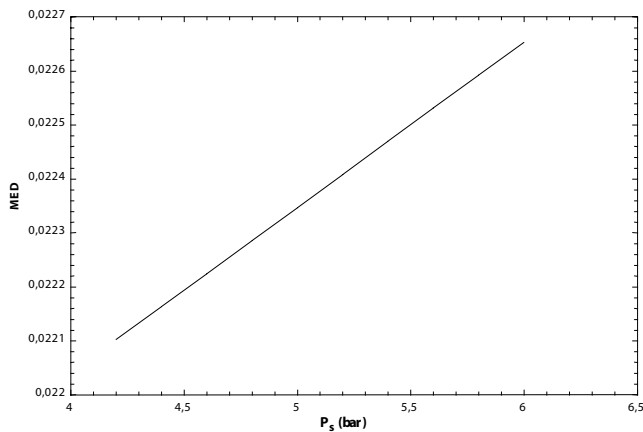


Fig. 19. Overall exergetic efficiency according to motive steam pressure.

This result agrees with the investigations of Almutairi et al. [3] performed on cogeneration power combined cycle and ME-TVC-MED water desalination plant. Also, Nafey et al. [23] obtained overall exergy efficiency of MSF process of about 1.87%.

5. Conclusion

Energetic and exergetic optimization of a DE-TVC (ME-TVC) desalination system is conducted in collaboration with the TCG.

The main objective of this study is to define the optimum operating conditions leading to the maximum exergy efficiency. For this purpose, the effects of the main operating parameters on the desalination unit performances and costs are analyzed. The following concluding remarks point out the major obtained results:

- The maximum exergy efficiency is obtained for the evaporator 2 (82%) followed by the distillate and brine pumps (80% and 78%). The condenser has the lowest exergy efficiency (31.66%).
- The total exergy destruction rate constitutes 73.3% of the provided exergy rate. The thermocompressor is the major contributor in exergy destruction of about 533.5 kW. This represents about 65% of the total exergy destruction rate.
- The mass flow rate \dot{m}_s and the pressure P_s of the motive steam affect positively the GOR, while the last one decreases slightly with the motive steam temperature T_s . This is due to the fact that a part of input heat flux is used for sensible seawater heating. In addition, the latent heat is reduced at higher temperatures.
- The specific heat transfer area decreases sensibly with \dot{m}_s .
- The exergy efficiency increases slightly with P_s while the production cost is practically constant. The two parameters decrease with T_s . For T_s higher than 154°C, the production cost becomes almost constant, while the exergy efficiency continues to decrease very slightly.
- In order to preserve suitable overall exergy efficiency with low production cost of distillate water, the motive steam temperature should be taken between 152°C and 154°C.

This corresponds to motive steam pressure between 4.4 and 4.7 bar. These ranges constitute optimum operating conditions.

These remarks constitute for the TCG decision criteria in order to better select the operating conditions of the desalination system in the aim to improve its performance.

Symbols

A	—	Area, m ²
BPE	—	Boiling point elevation
C_p	—	Specific heat, kJ/kg °C
D	—	Distillate mass flow rate, kg/s
\dot{E}	—	Exergy rate, kW
ER	—	Entrainment ratio
GOR	—	Gain output ratio
h	—	Specific enthalpy, kJ/kg
L	—	Latent heat, kJ/kg
\dot{m}	—	Mass flow rate, kg/s
P	—	Pressure, bar
Q	—	Heat flux, kW
R	—	Gas constant
s	—	Entropy, kJ/kg °C
sA	—	Specific heat transfer area, m ² s/kg
Sw	—	Seawater
T	—	Temperature, K
U	—	Overall heat transfer, kW/m ² °C
X	—	Salt weight percentage
x	—	Mass fraction

Greek

D	—	Difference
h	—	Efficiency

Subscripts

B	—	Brine
c	—	Saturation
cc	—	Condensation
cd	—	Condenser
ch	—	Chemical
D	—	Destruction
dis	—	Distillate
e	—	Exit
ev	—	Evaporator
F	—	Feed
G	—	Entrained vapor
i, in	—	Inlet, inside
is	—	isentropic
k	—	k_{th} element
ke	—	kinetic
M	—	Mixture
N	—	Condensate I
O, out	—	outlet
p	—	potential
ph	—	Physical
w	—	Work

References

- [1] S. Sadri, M. Ameri, R.H. Khoshkhoo, Multi-objective optimization of MED-TVC-RO hybrid desalination system based on the irreversibility concept, *Desalination*, 402 (2017) 97–108.
- [2] I.S. Al-Mutaz, I. Wazeer, Optimization of location of thermo-compressor suction in MED-TVC desalination plants, *Desal. Wat. Treat.*, 57 (2016) 26562–26576.
- [3] A. Almutairi, P. Pilidis, N. Al-Mutawa, M. Al-Weshahi, Energetic and exergetic analysis of cogeneration power combined cycle and ME-TVC-MED water desalination plant: Part-1 operation and performance, *Appl. Therm. Eng.*, 103 (2016) 77–91.
- [4] K.M. Bataineh, Multi-effect desalination plant combined with thermal compressor driven by steam generated by solar energy, *Desalination*, 385 (2016) 39–52.
- [5] B. Ortega-Delgado, P. Palenzuela, D.C. Alarón-Padilla, Parametric study of a multi-effect distillation plant with thermal vapor compression for its integration into a Rankine cycle power block, *Desalination*, 394 (2016) 18–29.
- [6] S. Azimibavil, A.J. Dehkordi, Dynamic simulation of a multi-effect distillation (MED) process, *Desalination*, 392 (2016) 91–101.
- [7] A. Al Ghamdi, I. Mustafa, Exergy analysis of a MSF desalination plant in Yanbu, Saudi Arabia, *Desalination*, 399 (2016) 148–158.
- [8] Y. Ghalavand, M.S. Hatamipour, A. Rahimi, Performance evaluation of humidification-compression desalination, *Desal. Wat. Treat.*, 57 (2015) 15285–15292.
- [9] M.T. Mazini, A. Yazdizadeh, M.H. Ramezani, Dynamic modeling of multi-effect desalination with thermal vapor compressor plant, *Desalination*, 353 (2014) 98–108.
- [10] I.S. Al-Mutaz, I. Wazeer, Comparative performance evaluation of conventional multi-effect evaporation desalination processes, *Appl. Therm. Eng.*, 73 (2014) 1194–1203.
- [11] O. Samaké, N. Galanis, M. Sorin, Thermodynamic study of multi-effect thermal vapour-compression desalination systems, *Energy*, 72 (2014) 69–72.
- [12] I.S. Al-Mutaz, I. Wazeer, Development of a steady-state mathematical model for MEE-TVC desalination plants, *Desalination*, 351 (2014) 9–18.
- [13] B. Han, Z. Liu, H. Wu, Y. Li, Experimental study on a new method for improving the performance of thermal vapor compressors for multi-effect distillation desalination systems, *Desalination*, 344 (2014) 391–395.
- [14] Y.D. Kim, K. Thu, A. Myat, K. Choon Ng, Numerical simulation of solar-assisted multi-effect distillation (SMED) desalination systems, *Desal. Wat. Treat.*, 51 (2012) 1242–1253.
- [15] F. Hafidhi, T. Khir, A.B. Yahyia, A.B. Brahim, Energetic and exergetic analysis of a steam turbine power plant in an existing phosphoric acid factory, *Energy Convers. Manage.*, 106 (2015) 1230–1241.
- [16] G. Tsatsaronis, Definitions and nomenclature in exergy analysis and exergoeconomics, *Energy*, 32 (2007) 249–253.
- [17] N. Shokati, F. Ranjbar, M. Yari, A comparative analysis of Rankine and absorption power cycles from exergoeconomic viewpoint, *Energy Convers. Manage.*, 88 (2014) 657–668.
- [18] H.T. El-Dessouky, H.M. Ettouney, *Fundamentals of Salt Water, Desalination*, Elsevier, Printed in the Netherlands, 2002.
- [19] S.E. Shakib, M. Amidpour, C. Aghanajafi, Simulation and optimization of multi-effect desalination coupled to a gas turbine plant with HRSG consideration, *Desalination*, 285 (2012) 366–376.
- [20] A.S. Nafey, H.E.S. Fath, A.A. Mabrouk, Thermoeconomic design of a multi-effect evaporation mechanical vapor compression (MEE-MVC) desalination process, *Desalination*, 230 (2008) 1–15.
- [21] Entropie Corporation Catalog ENT-C 2600, N/R A264/99393/DR, 09, 2000, p. 06.
- [22] F.N. Alasfour, M.A. Darwish, A.O.B. Amer, Thermal analysis of ME-TVC+MEE desalination systems, *Desalination*, 174 (2005) 39–61.
- [23] A.S. Nafey, H.E.S. Fath, A.A. Mabrouk, Exergy and thermoeconomic evaluation of MSF process using a new visual package, *Desalination*, 201 (2006) 224–240.